STRENGTH AND HYSTERETIC BEHAVIOR OF STEEL COLUMN-TO-FOOTING CONNECTION

B. Kato (I)
M. Morita (II)
A. Tanaka (III)
N. Fujita (IV)
Presenting Author: K. Morita

SUMMARY

This paper presents the mechanism of stress transfer, the maximum strength and the hysteretic behavior of the embedded type steel column-to-footing connections. The bearing stress between the footing concrete and steel column and the punching shear stress of the covering concrete of footing beam are calculated using an assumed stress transfer mechanism, and the fracture condition of the covering concrete is discussed. The effects of the experimental parameters on the hysteretic behavior of the column-to-footing connections are also discussed.

INTRODUCTION

Embedded type column-to-footing connections are often used in Japan, in order to connect steel columns with reinforced concrete footing beams rigidly. Some experimental studies were carried out when the steel column was embedded in the continuous footing beam (Ref. 1, 2). In this paper the mechanism of stress transfer, the fracture mode due to the punching shear stress, and the hysteretic behaviors of this type of column-to-footing connections are investigated experimentally for the case of exterior columns where the amount of concrete encasement is limited.

TEST SCHEME

Specimen A, B and C (CB test series) have diagonal bracings with rectangular hollow section connected to the steel columns of wide flange section at the column-to-footing connection, while Specimen D, E and F (CR test series) have no braces. Experimental parameters are: embedded length of steel column into the footing, the thickness of covering concrete from the flange of column to the side of footing, the arrangement of hoops and reinforcing bars around the embedded column and the stud connectors welded at the flange of column. The details are shown in Table 1 and Fig. 1.

The loading program is shown in Fig. 2. The maximum axial loads applied to the steel brace and the steel column were 75 tonf due to the capacity of loading equipment.

(I) Professor, Dr., The University of Tokyo

(II) Associate Professor, Dr., Chiba University

(III) Research Engineer, Dr., Technical Research Institute, Taisei Corporation

(IV) Graduate Student, Chiba University

TEST RESULTS AND DISCUSSION

Test Results

The mechanical properties of used materials are shown in Table 2. The relation between bending moment of steel column considering N_c-δ_s effect at the upper face of footing beam (M_F) and the deformations of the column which were measured at two levels of bases (δ_T, δ_s) are shown in Fig. 3. The stress distribution at the embedded part of steel column and the cracks appeared on the surface of footing concrete until the ultimate state of specimen are shown in Fig. 4 and Fig. 5 respectively. As shown in these figures, the covering concrete of Specimen C in case of positive loading (p.l.), and that of Specimen F in case of negative loading (n.l.) were fractured by punching shear. The ultimate strength of those specimens did not attain to the full plastic moment of steel column. As for the covering concrete of Specimen B, the punching shear cracks developed considerably, but it was not fractured until the specimen withstood the full plastic moment of steel column. The punching shear cracks did not develop so severely for Specimen A, D and E at the stage of full plastic moment of steel column.

Discussion

The assumed analytical model of stress transfer from steel column to footing beam is shown in Table 3, i.e. the stresses of steel column and steel brace are transfered to the footing concrete by bearing and friction between footing concrete and steel column, where the frictional coefficient is assumed as 0.5. The shearing resistance of stud connectors are also considered. The bearing stress-strain relationship for concrete is assumed as elastic-perfectly plastic for simplicity. The punching shear is assumed to develop as shown in Fig. 6 for positive and negative loading case respectively.

The stress distributions at the embedded part of steel column shown in Fig. 4 by solid line are calculated according to the equations of Table 3 neglecting the stress transfer by stud connectors, because they may be considered to become effective at the final stage of loading. The measured values coincide with the calculated values fairly well. The stress level of bearing stress between footing concrete and steel column corresponding to Table 3 and the calculated punching shear stress on the assumed punching shear plane (τ_p) at the maximum strength of each specimen are shown in Table 4. The calculated punching shear stress τ_p of the covering concrete of the specimens fractured by punching shear is $1.10\sqrt{F_c}$ for Specimen C in case of positive loading and $0.95\sqrt{F_c}$ for Specimen F in case of negative loading. And the assumed fracture mode of punching shear of those specimens corresponds well to the actual crack pattern shown in Fig. 5. The calculated τ_p of Specimen B in case of positive loading is $0.88\sqrt{F_c}$ which is almost the same value with that of Specimen F. But the covering concrete of Specimen B did not fracture until ultimate stage of loading because of heavy arrangement of hoops and reinforcing bars around the embedded column, although the punching shear cracks developed considerably. As for the other specimens where the development of punching shear cracks were only limited, the calculated τ_p are less than $0.61\sqrt{F_c}$. Considering the complex state of various stresses and heavy arrangement of hoops and reinforcing bars around the embedded column, these correspondence between τ_p and the state of punching shear cracks are fairly reasonalbe (Ref. 3).

CONCLUDING REMARKS

The punching shear fracture of the covering concrete of the embedded type steel column-to-footing connection can be estimated with the assumed analytical model. From the viewpoint of the hysteretic behavior, the maximum strength of this type of column-to-footing connections should exceed the full plastic strength of steel column. In order to satisfy this design criterion, the embedded length of column into the footing beam, the thickness of covering concrete from the flange of column to the side of footing beam and the arrangement of hoops and reinforcing bars should be designed carefully, considering the above mentioned punching shear fracture mode.

ACKNOWLEDGEMENT

The greater part of the experiments reported herein was carried out as one of the Japanese support tests of U.S.-Japan Cooperative Research Program Utilizing Large Scale Testing Facilities. The writers wish to thank Y. Yokoyama, graduate student of Chiba University, and S. Minewaki, Takenaka Komuten Co., for their contributions to the research efforts.

Table 1 Experimental Parameters of the Test Specimen

Test Series	CB			CR		
Test Specimen	A	B	C	D	E	F
Thickness of Covering Concrete (t)*(cm)	33.8 34.7	23.9 24.7	14.7 14.7	16.5 14.7	13.2 14.7	14.5 15.0
Embedded Length of Steel Column (d)(cm)	60	40	40	40	30	36.3
Stud Connectors Welded at Each Flange of Column	6-ϕ16	6-ϕ16	6-ϕ16	6-ϕ16	6-ϕ16	—

* Upper Row — Measured Value, Lower Row — Schemed Value

Table 4 Results of Analysis

		A	B	C	D	E	F
Maximum Strength (p.l.)	M_F(tf·m)	14.49	13.10	9.89	12.24	13.04	7.71
	Q_C(tf)	7.00	6.71	5.43	5.84	6.01	4.50
	Q_B(tf)	52.60	50.10	52.70	—	—	—
Stress Level		(1)	(1)	(1)	(1)	(1)	(2)
$\tau_p/\sqrt{F_c}$		0.61	0.88	1.10	0.29	0.45	0.60
Maximum Strength (n.l.)	M_F(tf·m)	-14.86	-14.57	-13.08	-12.64	-15.21	-7.63
	Q_C(tf)	-12.00	-13.60	-10.86	-10.35	-14.00	-5.20
	Q_B(tf)	-53.03	-53.10	-53.17	—	—	—
Stress Level		(1)	(3)	(3)	(1)	(1)	(3)
$\tau_p/\sqrt{F_c}$		0.23	0.41	0.41	0.23	0.54	0.95

$\tau_p = N_{fu}/A_p$ in case of positive loading
$\tau_p = N_{f\ell}/A_p$ in case of negative loading

Table 2 Mechanical Properties of Used Materials

	Yield Stress σ_y (kgf/mm^2)	Tensile Strength σ_B (kgf/mm^2)	Elongation EL. (%)
Column Flange	27.4 (34.3)*	45.2 (51.8)	30.9 (27.7)
Web	34.1 (36.6)	46.8 (54.6)	23.3 (22.9)
Brace	27.7 (—)	45.0 (—)	29.1 (—)
Reinforcing D22	35.9 (37.9)	53.8 (57.6)	17.9 (22.0)
Bar D10	37.8 (37.2)	54.4 (57.6)	19.1 (21.3)
Stud Connector	39.2 (—)	48.1 (—)	36.7 (—)
Concrete	Young's Modulus E_c(kgf/cm^2) 2.14×10^5 (1.60×10^5)		
	Compressive Strength F_c(kgf/cm^2) 247 (176)		

* ( ) — Value for Specimen F

Table 3 Analytical Model of Stress Transfer and Equation of Equilibrium

Stress Level		Equation of Equilibrium
	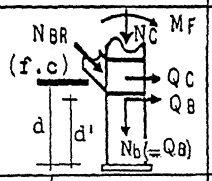	(Shear) $N_{fu}-N_{f\ell}=Q_C+Q_B$ (Moment) $M_c+M_{fr}+M_b+M_s=M_F+Q_Cd+Q_Bd'$ $M_{fr}=\pm H(N_{fu}+N_{f\ell})/4$ $M_s=\pm n_{sc}a\sqrt{E_cF_c}\,H/2$
(1)	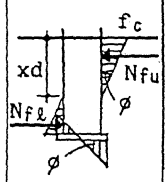 ($f_c \leqq F_c$)	$N_{fu}=\pm bf_c\,dx/2$ $N_{f\ell}=\pm bf_c\,d(1-x)^2/2x$ $M_c=\pm bf_c\,d^2x(1-x/3)/2\mp bf_c\,d^2(1-x)^3/6x$ $M_b=\pm wh^3\phi/12$ $\phi=f_c/dx$ $f_b=\pm N_b/wh+\phi h/2$ $N_b=N_c+Q_B\mp(N_{fu}-N_{f\ell})/2$ ($N_b \geqq whF_c \longrightarrow M_b=0$)
(2)	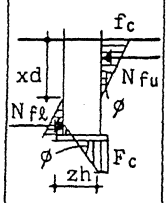	$N_{fu}=\pm bf_c\,dx/2$ $N_{f\ell}=\pm bf_c\,d(1-x)^2/2x$ $M_c=\pm bf_c\,d^2x(1-x/3)/2\mp bf_c\,d^2(1-x)^3/6x$ $M_b=\pm wh^2F_c\,z(1-z)/2\mp whz(2F_c-\phi hz)(h/2-zh(3F_c-\phi hz)/3(2F_c-\phi hz))/2$ $\phi=f_c/dx$ $z=\sqrt{(2whF_c-2N_b)/wh^2\phi}$ $N_b=N_c+Q_B\mp(N_{fu}-N_{f\ell})/2$
(3)	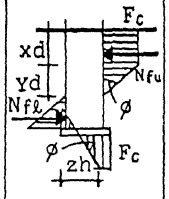	$N_{fu}=\pm bF_c\,dx\pm bF_c\,dY/2$ $N_{f\ell}=\pm bF_c\,d(1-x-Y)^2/2Y$ $M_c=\pm bF_c\,d^2x(1-x/2)\pm bF_c\,d^2Y(1-x-Y/3)/2\mp bF_c\,d^2(1-x-Y)^3/6Y$ $M_b=\pm wh^2F_c\,z(1-z)/2\mp whz(2F_c-\phi hz)(h/2-zh(3F_c-\phi hz)/3(2F_c-\phi hz))/2$ $\phi=F_c/dY$ $z=\sqrt{(2whF_c-2N_b)/wh^2\phi}$ $N_b=N_c+Q_B\mp(N_{fu}-N_{f\ell})/2$ ($N_b \geqq whF_c \longrightarrow M_b=0$)

Remarks

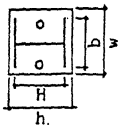

n : Number of stud connectors at each flange
$_{sc}a$: Sectional area of a stud connector
M_b, N_b : Moment, axial force transferred by bearing between footing concrete and base plate
* : Upper sign for positive loading and lower sign for negative loading

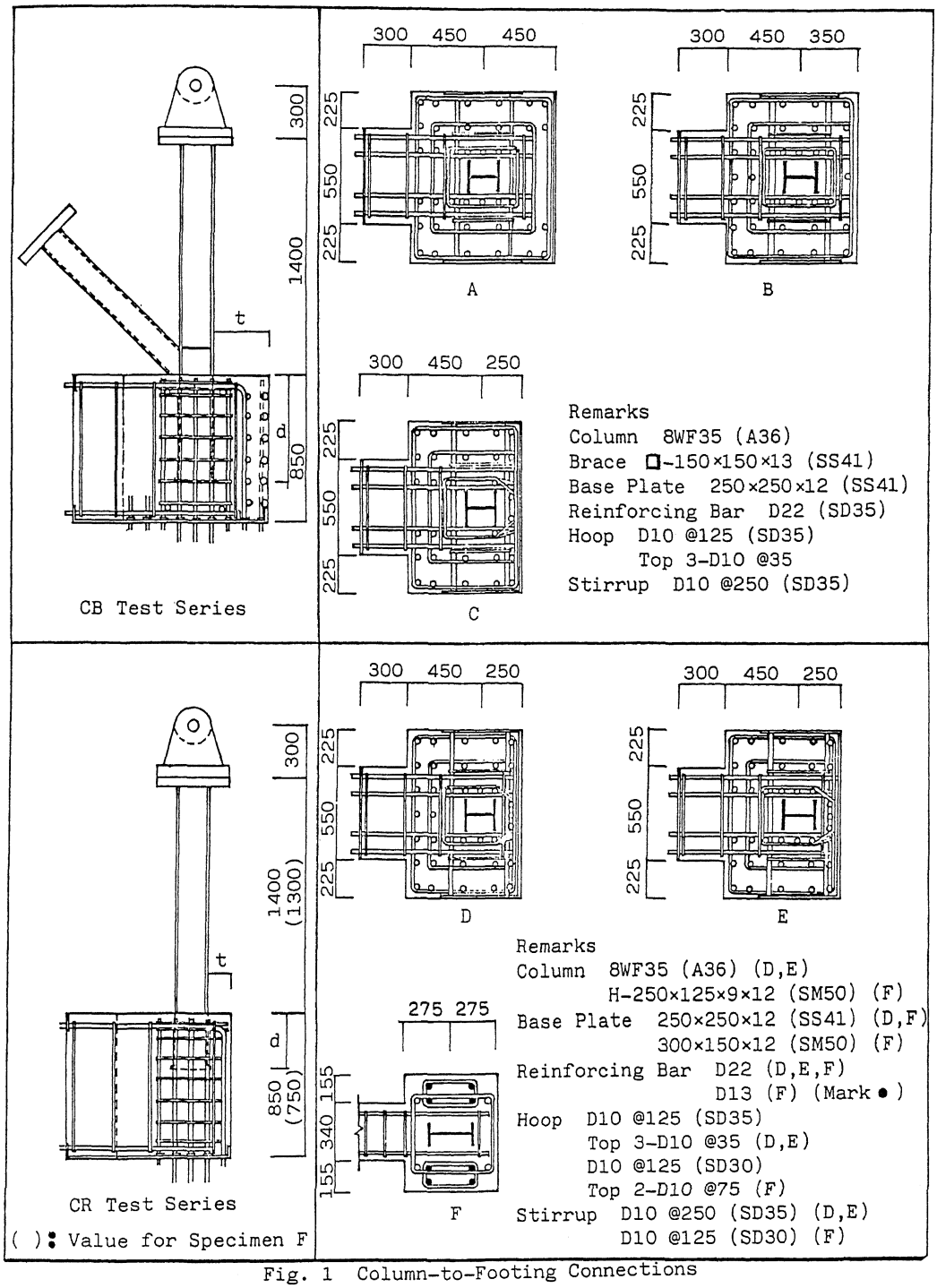

Fig. 1 Column-to-Footing Connections

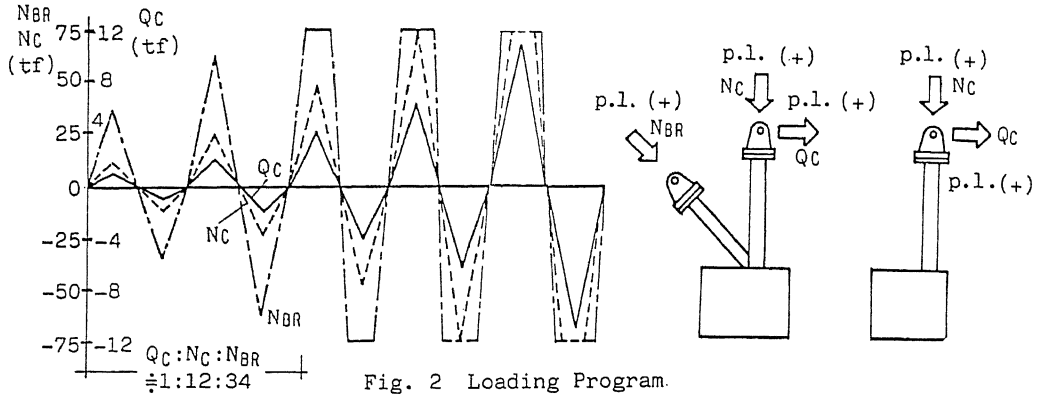

Fig. 2 Loading Program

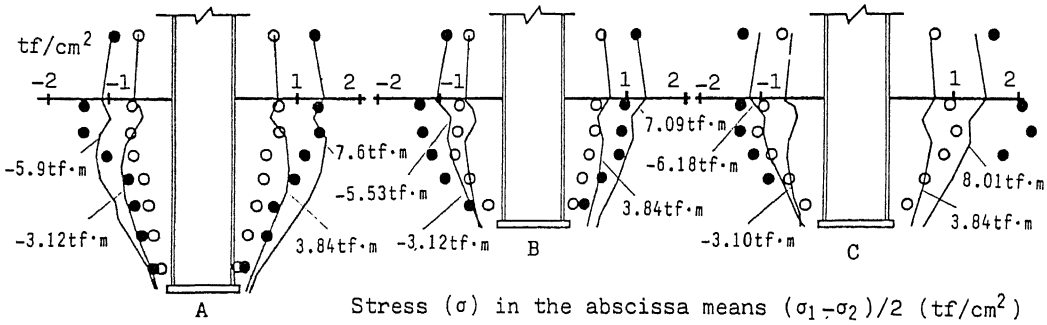

Stress (σ) in the abscissa means $(\sigma_1 - \sigma_2)/2$ (tf/cm^2)

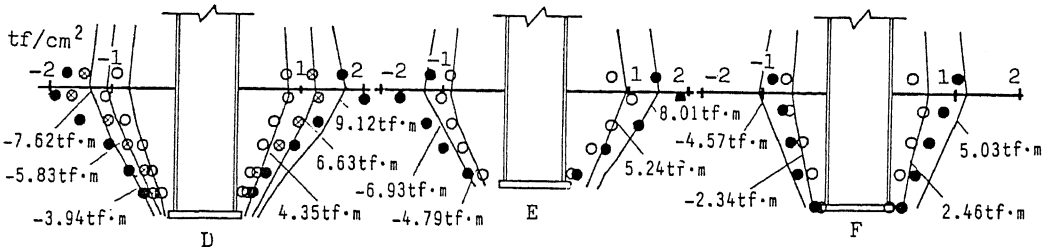

Solid Line —— Calculated Value

Mark " ○ , ⊗ , ● " —— Measured Value

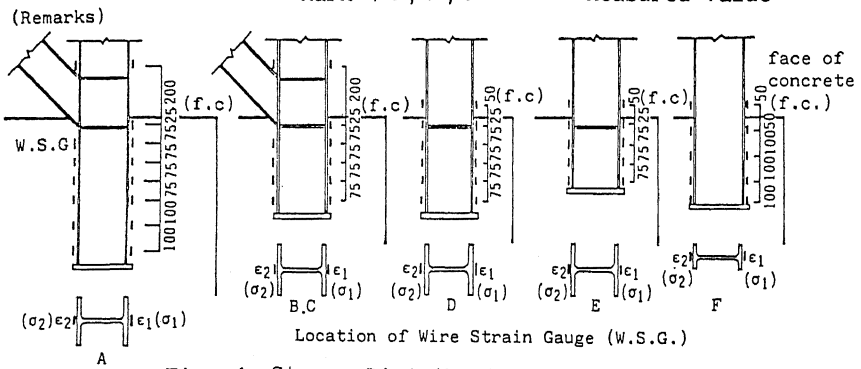

Fig. 4 Stress Distribution of Steel Column

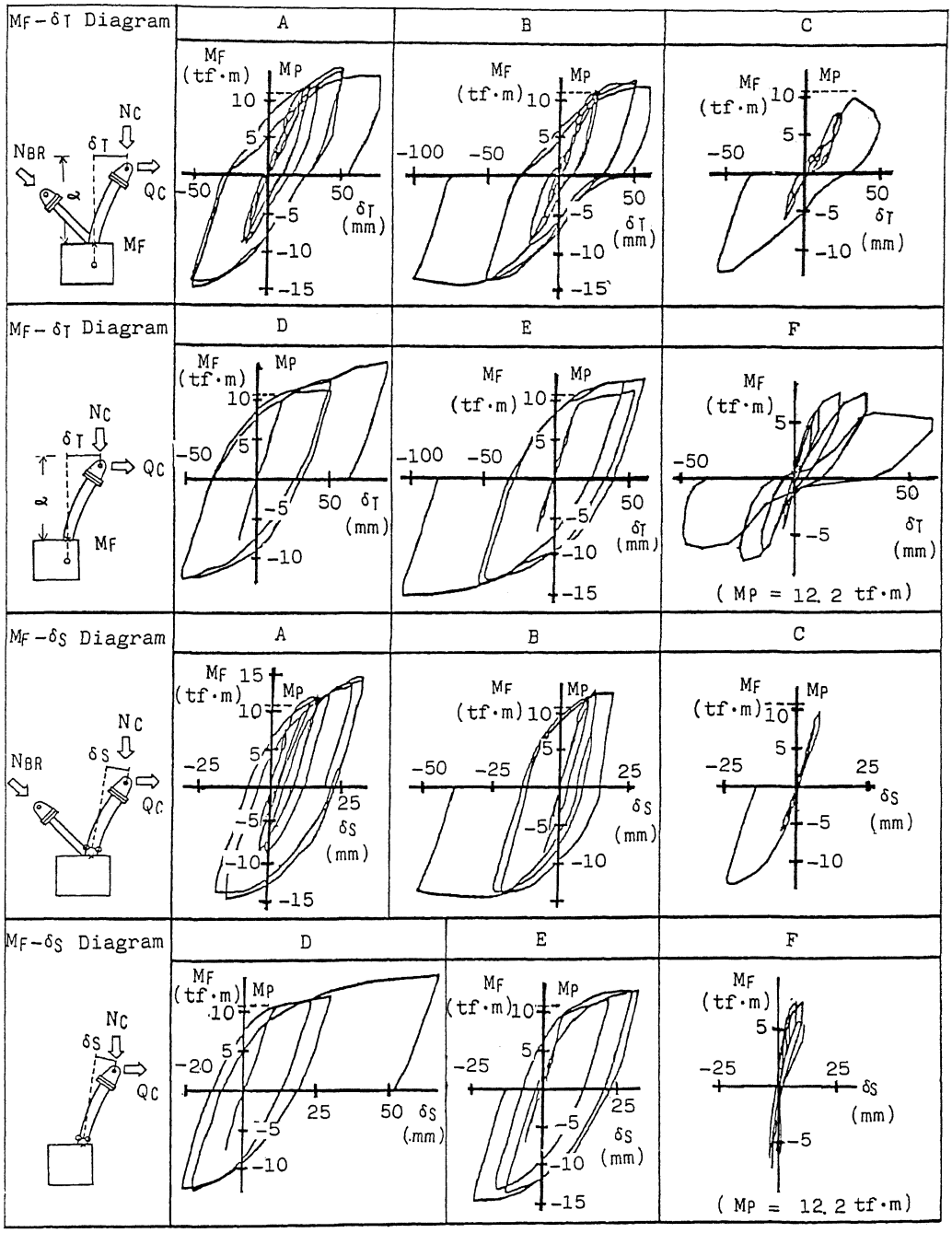

Mp : Full Plastic Moment of Steel Column

$M_F = Q_C \cdot \ell + N_C \cdot \delta_s$

Fig. 3 Mf-δ Diagram for Joint

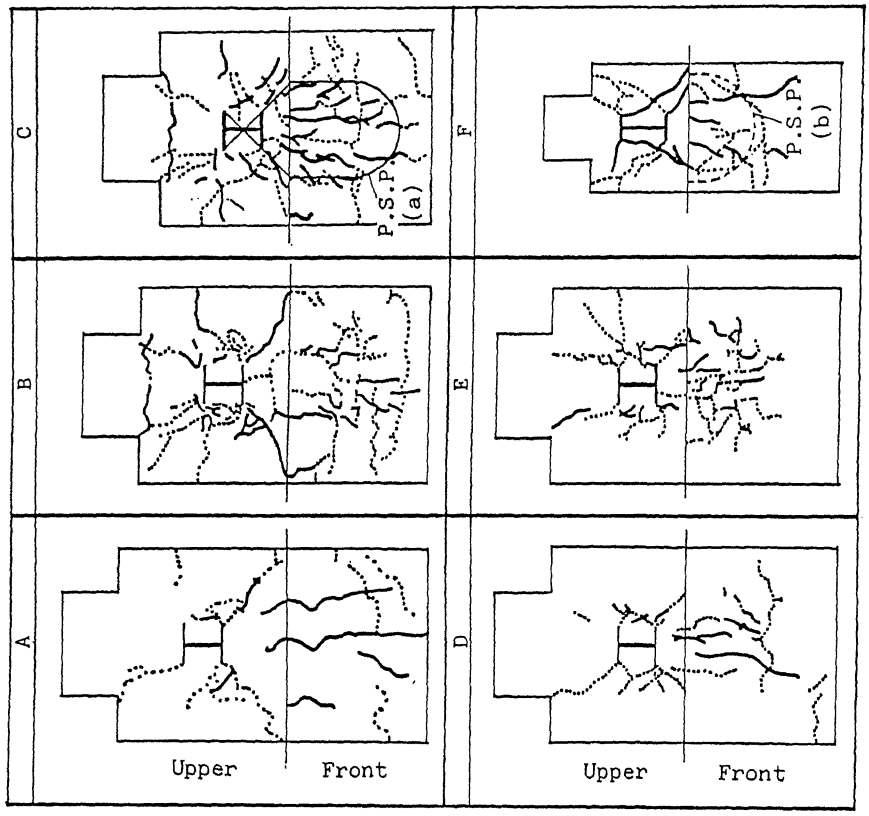

Solid lines···Cracks opened at positive loading
Dotted lines···Cracks opened at negative loading

Fig. 5 Crack Pattern

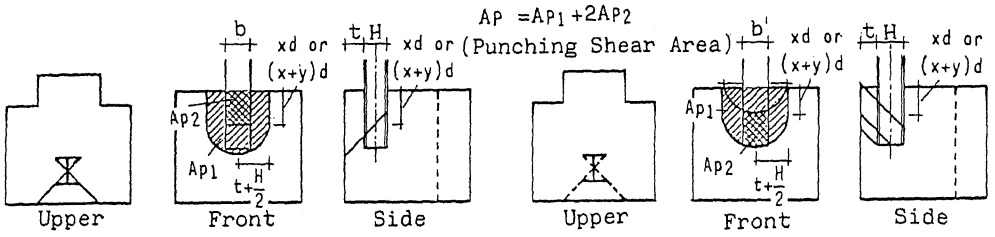

(a) Positive Loading Case (b) Negative Loading Case

Fig. 6 Punching Shear Plane (P.S.P.)

REFERENCES

1. K. Washio, T. Suzuki, et al. "ON THE EMBEDDED EFFECT OF STEEL COLUMN INTO FOOTING BEAM AT THE STEEL COLUMN-TO-FOOTING CONNECTIONS" ABSTRACTS, ANNUAL MEETING OF AIJ, SEPTEMBER (1978)

2. H. Akiyama, M. Kurosawa, et al. "STRENGTH AND DEFORMABILITY OF EMBEDDED TYPE STEEL COLUMN-TO-FOOTING CONNECTIONS" ABSTRACTS, ANNUAL MEETING OF AIJ, SEPTEMBER (1981)

3. ACI CODE REQUIREMENTS FOR NUCLEAR SAFETY RELATED CONCRETE STRUCTURES (ACI 349-76)